

# Reliability of InGaP-Emitter HBTs

Bob Yeats, Paul Chandler, Morgan Culver, Don D'Avanzo, Gilbert Essilfie, Craig Hutchinson, David Kuhn, Tom Low, Tim Shirley, Sunil Thomas, Wes Whiteley

Agilent Technologies, 1412 Fountaingrove Parkway, Santa Rosa CA, 95403, bob\_yeats@agilent.com, (707)577-4076

## ABSTRACT

Various reliability results are discussed for Agilent's InGaP-emitter HBTs. The MTTF distribution for 30 wafers, stressed at the severe stress of  $T_J = 334^\circ\text{C}$  and  $J_E = 1.8 \text{ mA}/\mu\text{m}^2$ , has a median value of 1159 h. Activation energy ( $E_A$ ) and current density acceleration exponent ( $n_j$ ) have been measured on discrete HBTs for 6 wafers in the early-to-fail part of this MTTF distribution. We consistently found  $E_A \approx 1.2 \text{ eV}$ , while  $n_j$  could be determined only crudely ( $\sim 1.2$ ) due to the limited range of current density used. Wafers with intentional lattice mismatch in the InGaP layer were found to be consistent with this same (nominally lattice matched) MTTF distribution, although a wafer with the largest Ga-rich mismatch had among the best lifetimes (85<sup>th</sup> percentile). The failure mode that predominates in our devices is sudden  $\beta$  degradation to  $\beta \approx 1$ . The large base currents triggered by device failure enable MSI-level reliability test circuits to be designed that are sensitive to failure of a single transistor. Such circuits are being used to explore the threat of infant failures in large circuits. Base current appears to be a more general indicator than emitter current for the MTTF current acceleration factor, as the large base currents that can occur in saturation are found to have a base current acceleration exponent of  $n_{J_B} \approx 1.8$ .

## INTRODUCTION

InGaP-emitter HBTs have received much attention in the last several years because they have much better reliability than AlGaAs-emitter HBTs [1-7]. InGaP HBTs can have a number of different failure modes [2,3,4,7], but when the fabrication process is optimized, it appears that the fundamental failure mode is sudden and drastic  $\beta$  (DC current gain) degradation. This failure mode has a relatively low activation energy, and devices can survive extremely long times under the most severe stresses. This durability has inhibited the study of the temperature and current density stress acceleration parameters ( $E_A$ ,  $n_j$ ). In this work we report the results of lengthy HTOL measurements of InGaP HBTs for over 30 wafers. Only the wafers with relatively poor reliability have MTTFs that are short enough (though still very long) to make practical the determination of  $E_A$  and  $n_j$ . Even these poorer wafers were found to have projected lifetimes at  $T_J = 150^\circ\text{C}$  and  $J_E = 0.6 \text{ mA}/\mu\text{m}^2$  exceeding  $10^6 \text{ h}$ .

We have also studied whether intentional lattice mismatch in the InGaP emitter layer affects reliability. Based on a small sample size, it appears that for the expected range of lattice mismatch in vendor material, lattice mismatch does not significantly affect reliability. In fact, there may even be a beneficial effect of mismatch on the Ga-rich side.

## DEVICE FABRICATION

A schematic cross section of our InGaP-emitter HBT is shown in Fig. 1. The epitaxial material is manufactured by Kopin Corp.[6] using OMVPE. The device structure features alloyed collector contacts, a 400 nm collector drift region, an 80 nm carbon doped base, an InGaP emitter, and a highly doped InGaAs contact layer. The process utilizes G-line stepper lithography that readily defines the minimum geometries,  $2 \times 2 \mu\text{m}$  emitters and  $1 \times 1 \mu\text{m}^2$  vias.  $\text{SiCl}_4$  based RIE is used to define the emitter mesa, emitter ledge/base contact, and the base-collector mesa. Polyimide is used for the interlayer dielectric. Other important features include a non-alloyed  $n^+$  InGaAs emitter contact, a non-alloyed base contact, a depleted InGaP passivation ledge, PECVD SiN passivation, and He implant [8,9] for isolation. These HBTs are biased at up to  $0.6 \text{ mA}/\mu\text{m}^2$  in normal operation. Typical transistor parameters include  $F_t = 65 \text{ GHz}$ ,  $F_{\text{MAX(MAG)}} = 75 \text{ GHz}$ ,  $\beta = 132$ ,  $BV_{\text{CEO}} = 8.3 \text{ V}$ , and  $BV_{\text{CBO}} = 15 \text{ V}$ .

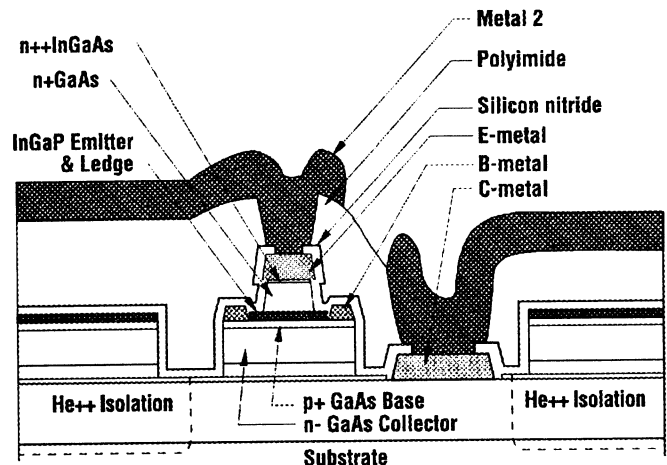


Fig. 1. Schematic cross-section of InGaP emitter HBT.

## RELIABILITY RESULTS

Our previously reported reliability work was based on Darlington amplifier circuits. More recently we have been focusing on the reliability of discrete HBTs. We have used two different types of discrete HBT reliability test chips. Initially, reliability was investigated using a chip having a single  $2 \times 4 \mu\text{m}^2$  HBT. These chips were bonded up 8 to a

package, and the packages were subjected to high temperature stress under bias. At intervals, the stress was interrupted, the packages were removed from the heating fixture, and a variety of transistor parameters were measured at room temperature so that parameter drift could be monitored. It was observed in these tests that the failure mechanism involved  $\beta$  drift only; i.e., contacts, leakage currents, resistances, and forward voltages were stable.

This led us to develop an alternative highly automated test system. In this test system, the stress is *never* interrupted for parameter measurements. Instead bias voltages and currents are monitored *at the stress condition* by computer control, and data is saved to a database (typically at 10 times per decade of time). This method allows the key drifting parameter  $\beta$  to be automatically monitored. Furthermore, handling is eliminated so the quality of the reliability data is greatly improved (there are much fewer spurious results to consider). We will refer to this HTOL test system as the *automated* reliability test system. In the *automated* HTOL system we usually use a different kind of reliability test chip. The chip has four  $2 \times 4 \mu\text{m}^2$  HBTs that can be separately monitored for base current, as shown in Fig. 2. The 500 ohm emitter resistors allow stable bias at constant emitter current. By using common leads for the collectors and emitters, we can double the number of HBTs that fit in a package.

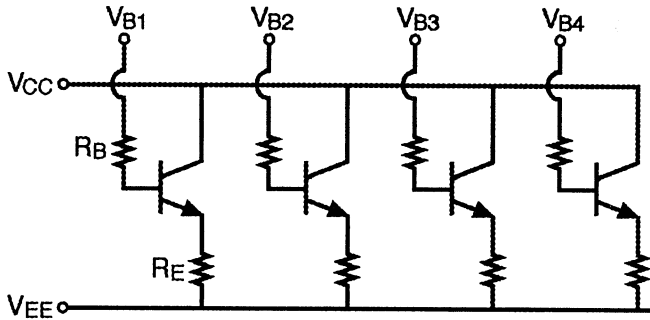


Fig. 2. Reliability test chip used in the *automated* HTOL system.  $R_E = 500 \Omega$ ,  $R_B = 50 \Omega$ .

We have obtained similar MTTFs at  $T_J \sim 330^\circ\text{C}$  for a given wafer for both types of reliability test chips and HTOL systems. Junction temperatures are carefully modeled, including the effects of topside metal, and the results have been verified by electrical measurements [10]. (Note: For comparing our results to others, one should be aware that we give *peak* rather than *average* junction temperatures. Our peak temperature of  $334^\circ\text{C}$  corresponds to an average junction temperature of  $307^\circ\text{C}$ . Here *average* refers to an average over the junction area in a horizontal cross-section that includes the hottest spot.)

Wafers are generally given a standard reliability stress on the *automated* HTOL system that consists of 500 h (or more) at  $T_J = 334^\circ\text{C}$  and  $J_E = 1.8 \text{ mA}/\mu\text{m}^2$ , which is quite severe compared to the nominal maximum use condition ( $150^\circ\text{C}$ ,

$0.6 \text{ mA}/\mu\text{m}^2$ ). The normalized  $\beta$  drift for a randomly selected sample of 500 devices from 30 wafers is shown in Fig. 3a, and a blow up of the low  $\beta$  region (unnormalized) is shown in Fig. 3b.  $\beta$  initially drops typically 5–25% in the first few hours, then sometimes *partially* recovers, and then remains unchanged for a long time until just before the device fails. The device failure is very rapid once it begins to fail, but is not instantaneous. At small times the spacing of measurement times is short enough to see (in a blow up of Fig. 3a, not shown) that  $\beta$  drops *continuously* to a final value of  $\sim 1$ . Figure 3b shows that all failed devices drift to a final value of  $\beta \approx 1$ , which represents complete collapse of a Gummel plot to  $I_B = I_C = I_E/2$ . For a large number of devices in Fig. 3 the stress was terminated before failure, so those traces end without a jump downward in  $\beta$ . The temperature dependence of  $\beta$  is rather weak: the initial  $\beta$  at  $334^\circ\text{C}$  is about 65% of the room temperature value.

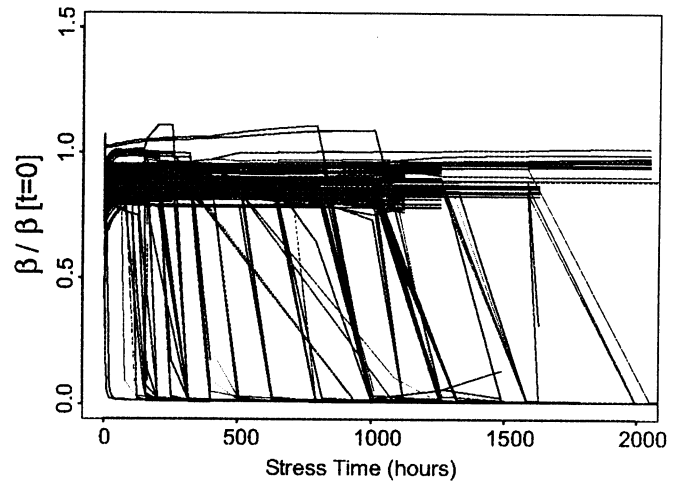


Fig. 3a. Normalized  $\beta$  drift at  $334^\circ\text{C}$  and  $1.8 \text{ mA}/\mu\text{m}^2$  for 500 HBTs. The important failure mechanism is the sudden drop in  $\beta$ .

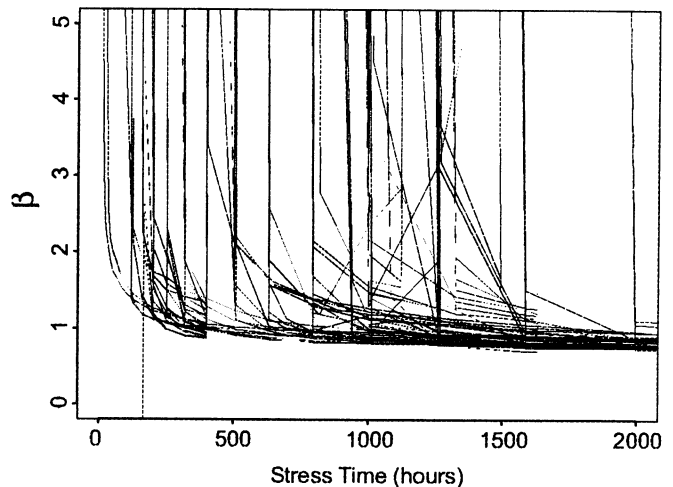


Fig. 3b. Expanded scale (unnormalized) showing that  $\beta$  of failed devices approaches one.

The drift for one of our best *AlGaAs*-emitter wafers is shown in Fig. 4. It differs from our InGaP-emitter results (Fig. 3) in that drift occurs at much lower stresses ( $T_J = 280^\circ\text{C}$ ,  $J_E = 0.6 \text{ mA}/\mu\text{m}^2$ ), and that there is a region where  $\beta$  gradually drifts downward prior to the eventual rapid  $\beta$  degradation near device failure. For our InGaP-emitter HBTs, there usually is no gradual downward drift region, instead  $\beta$  remains flat (however this is probably not the case for all InGaP HBT processes).

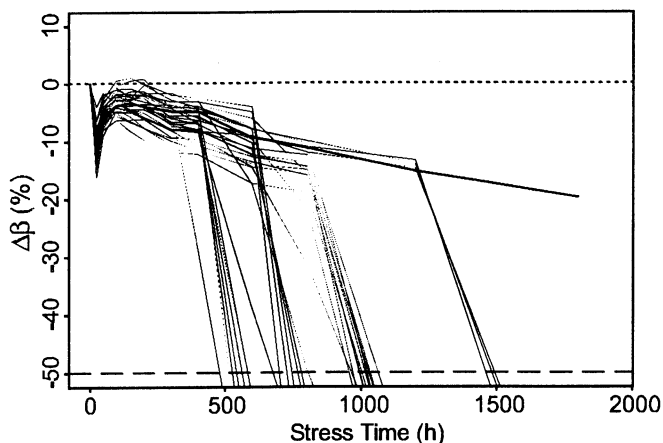


Fig. 4.  $\beta$  drift at  $T_J=280^\circ\text{C}$ ,  $J_E=0.6 \text{ mA}/\mu\text{m}^2$  for a good AlGaAs-emitter wafer.

If one takes Fig. 4 as the general case for  $\beta$  drift, there are three separate drift mechanisms. 1) There is the initial limited drift that partially recovers (this has often been attributed to grown in hydrogen [8,9]). 2) There is the gradual drift (absent in our InGaP HBTs), and 3) there is the large sudden  $\beta$  drop. Drifts of even 50% in  $\beta$  do not affect most circuits as long as  $\beta$  is large enough (e.g.,  $> 60$ ), so the first drift mechanism is regarded as an acceptable nuisance and will probably improve as epi and process technologies mature. The second drift mechanism (gradual drift) is usually not present in our process for InGaP, and we regard it as a solvable problem, probably associated with material, epi structure, or processing conditions. The third failure mechanism (sudden  $\beta$  drop) we regard as the fundamental or intrinsic failure mode for these HBTs. There is no correlation between the gradual drift region and the sudden  $\beta$  drop region: one cannot extrapolate from the gradual drift region to anticipate when a sudden  $\beta$  drop will occur.

We will analyze our reliability data for the sudden  $\beta$  drop failure mechanism. Operationally this is easy to do simply by choosing a large percentage (e.g. 50%) for a  $\beta$  drift failure criterion. One must be careful in interpreting published reliability results to see which failure mechanism they pertain to. There are a number of reports that pertain to gradual drift (e.g., failure criteria of  $\Delta\beta = 10$  or 20%), and large lifetimes projected from such data do not insure that reliability is acceptable with regard to the sudden  $\beta$  drop failure mechanism.

Figure 5 shows the MTTF distribution for a recently completed group of 30 wafers. These wafers were stressed very severely:  $T_J = 334^\circ\text{C}$ ,  $J_E = 1.8 \text{ mA}/\mu\text{m}^2$ . The MTTFs ranged between 260 h and  $> 3000$  h. Not shown on the plot is a wafer stressed for over 6000 h with only 1 out of 31 devices failing. The median MTTF is 1159 h and has a natural log sigma of 0.68. Most of the wafers in Fig. 5 are

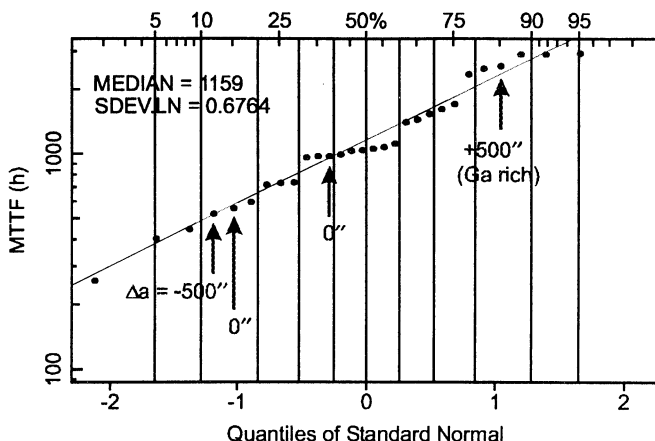


Fig. 5. MTTF distribution for 30 InGaP-emitter wafers stressed at  $T_J=334^\circ\text{C}$  and  $J_E = 1.8 \text{ mA}/\mu\text{m}^2$ . Four of the wafers have intentional lattice mismatch, as indicated.

nominally lattice matched (i.e., Kopin targets their growths at a slight mismatch of  $\Delta a \approx +100''$ , as measured on an occasional test wafer by  $\langle 400 \rangle$  rocking curve xray diffraction). However there were 4 wafers grown with intentional mismatch of  $-500''$ ,  $0''$ , or  $+500''$ ; these values were chosen to easily cover the extremes of the expected range of epi variability. Figure 5 shows that these intentionally mismatched wafers fit in the same distribution as the normal wafers. Hence, we are relieved to see that exact lattice match is not critical for good reliability. Furthermore, the wafer with the greatest positive mismatch ( $+500''$ , which is Ga-rich) had among the best MTTFs (the 85<sup>th</sup> percentile). So one might even speculate that it is beneficial for the InGaP to be Ga-rich.

To project the MTTFs of Fig. 5 to normal operating conditions we need to determine  $E_A$  and  $n_J$  ( $\text{MTTF} \sim J^{-n_J} \exp[E_A/kT_J]$ ). This requires use of several different stress conditions, but we hesitate to use stresses more severe than those used in Fig. 5. Lesser stresses require longer times to reach MTTF, which starts to be impractical for the long MTTFs in Fig. 5. The work-around used was to analyze 6 of the worst wafers of Fig. 5 so that MTTFs could be measured in practical times. All wafers in Fig. 5 appear to be part of the same distribution, so this approach is expected to give results that apply more broadly. Typical  $T_J$ 's used were between  $300^\circ\text{C}$  and  $334^\circ\text{C}$ , and  $J_E$ 's were between 1.2 and  $1.8 \text{ mA}/\mu\text{m}^2$ . An example of the data and fit for one of the wafers is shown in Fig. 6. The lines represent fitted results (constrained to constant sigma). The distribution of  $E_A$  for

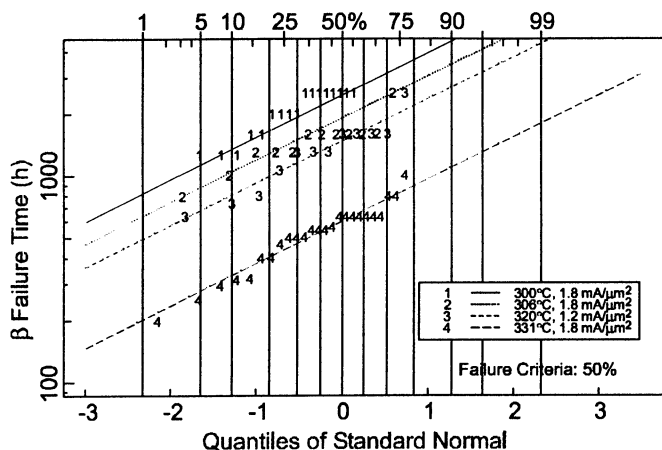


Fig. 6. Distribution of failure times at various stresses for a relatively poor InGaP-emitter wafer. Fitted results (lines) have  $E_A = 1.38$  eV,  $n_J = 1.07$ ,  $\sigma = 0.47$ , and  $MTTF = 1.7 \times 10^8$  h at  $150^\circ\text{C}$ ,  $0.6 \text{ mA}/\mu\text{m}^2$ .

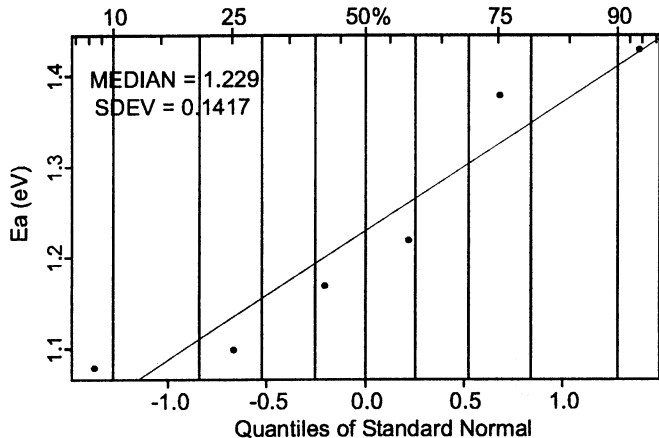


Fig. 7. Distribution of  $E_A$  for 6 InGaP-emitter wafers.

the 6 wafers is shown in Fig. 7. Values are consistently between 1.1 and 1.4 eV. These values are somewhat higher than values we have previously reported for amplifier circuits [4,5]. The discrepancy may be due to reduced handling in the *automatic* HTOL system, to small sample sizes in the earlier work, or to better knowledge of the temperature and current for a discrete HBT than for the transistor most at risk in the amplifier circuits. While these  $E_A$  values are *lower* than some reported by others [1,3], the lifetimes at a fixed stress are considerably *longer*. It is possible that other failure mechanisms could be occurring that promote the earlier failures and obscure a lower activation energy mechanism. Ueda et al. [2] have reported activation energies of 1.37 or 2.00 eV, depending on the base-electrode structure. They have also reported [2] two types of anomalies in failed devices: carbon precipitates in the base, and Au or Zn in the base (diffused from the base electrode). Our AlGaAs-emitter HBTs have lower  $E_A$  ( $\approx 0.7$  eV) than our InGaP-emitter HBTs. A fit for the AlGaAs-emitter HBT wafer of Fig. 4 is shown in Fig. 8; projected

MTTF at  $150^\circ\text{C}$ , and  $0.6 \text{ mA}/\mu\text{m}^2$  is only 105 kh. This was for one of our highest reliability AlGaAs-emitter HBT wafers.

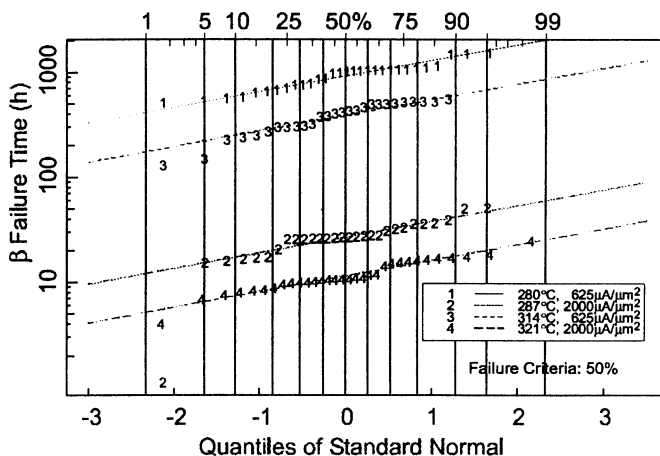


Fig. 8. AlGaAs-emitter HBT distribution of failure times for one of our best AlGaAs wafers. Fitted results (lines) have  $E_A = 0.72$  eV,  $n_J = 2.87$ ,  $\sigma = 0.34$ , and  $MTTF = 105$  kh at  $150^\circ\text{C}$ ,  $0.6 \text{ mA}/\mu\text{m}^2$ .

The values of  $n_J$  for the wafers of Fig. 7 varied between 0.1 and 2.9 (mean = 1.23, standard deviation = 0.99). Most of the variation of  $n_J$  is thought to be due to extraction errors rather than representing real variation. With a fairly high  $E_A$ , unaccounted for temperature variation can all too easily mask the effect of the relatively small range of current density used here (1.5:1). With a worst case value of  $n_J = 0$ ,  $10^6$  h at  $150^\circ\text{C}$  corresponds to 47 h at  $334^\circ\text{C}$  for  $E_A = 1.2$  eV. Hence all the wafers of Fig. 5 easily meet a  $10^6$  h MTTF requirement at  $150^\circ\text{C}$ . With  $E_A = 1.2$  eV, the median MTTF of 1159 h in Fig. 5 projects to 25 Mh (or 100 Mh) at  $150^\circ\text{C}$  and  $J_E = 0.6 \text{ mA}/\mu\text{m}^2$ , depending on whether  $n_J = 0$  (or 2), respectively. These lifetimes are long enough that more aggressive design limits for temperature or current density could be used.

The question arises whether emitter current or base current is a better indicator of current acceleration. Normally these currents are so highly correlated (through  $\approx$  constant  $\beta$ ), that the question is academic. However, if one *forward* biases the *collector*-base junction (which occurs naturally in saturation), one can independently set both  $I_B$  and  $I_E$ . One finds that  $MTTF \sim I_B^{-n_J}$  at constant  $I_E$ , with  $n_J \approx 1.8$ . If  $E_A = 1.2$  eV, then  $J_B < \sim 10 \mu\text{A}/\mu\text{m}^2$  seems to be required for  $10^6$  h MTTF at  $150^\circ\text{C}$ . So heavily saturated operation is undesirable for high reliability. Evidently, recombination in the base promotes defect formation and growth. Base current is a measure of such recombination. With base current driving reliability,  $\beta$  drop is more sudden due to a runaway effect: As the device begins to fail  $I_B$  increases; the increased  $I_B$  represents greater stress, which causes greater  $I_B$ , which causes greater stress, etc.

We now address the possibility of infant failures. The raw (individual device) data for the 30 wafers of Fig. 5 is plotted in Fig. 9. The data is a little skewed because not all of the devices have been stressed to failure. However, one notices that ~ 1% of the devices failed unusually early, as if there may have been an initial defect present in the device before stress. Since the stress was fully automated, there is less likelihood that handling caused these "infant" failures.

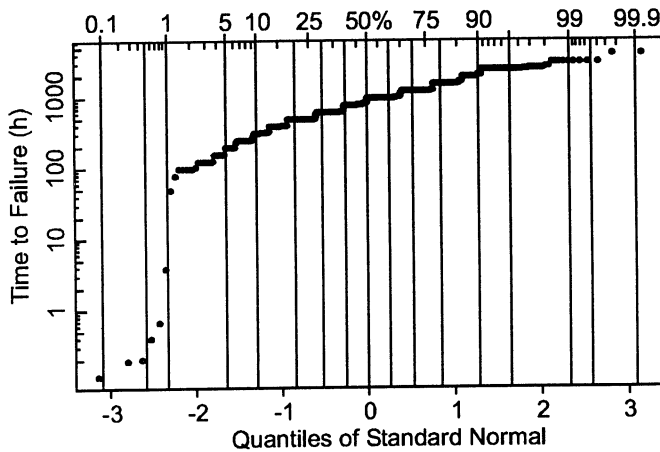


Fig. 9. Failure time distribution for 50%  $\beta$  drift for 832 individual devices from 30 InGaP-emitter wafers. Devices were stressed at  $T_J = 334^\circ\text{C}$  and  $J_E = 1.8 \text{ mA}/\mu\text{m}^2$ . About 1% of the devices fail in "infancy".

However, latent damage introduced in assembly might have caused them. If such assembly damage caused the infant failures, then there is not a fundamental problem, and large circuits might have a ~1% infancy failure rate, barring improved assembly. However, if the infant failures are due to uniformly distributed defects initially present in the wafer, then most circuits with > 100 transistors would fail in infancy (but not at final test). This would be unacceptable. A reliability test circuit to quantify infant failures has been designed (Fig. 10). In this circuit all the transistors are

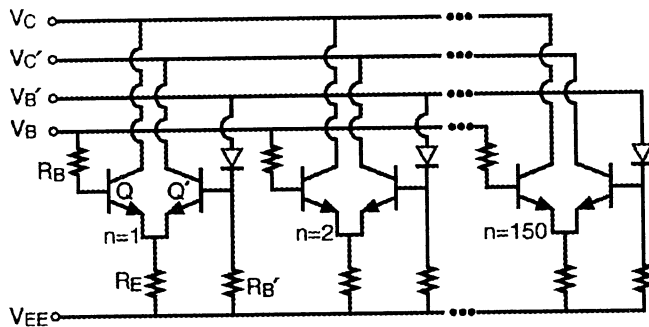


Fig. 10. Circuit schematic for large reliability test circuit sensitive to the failure of a single transistor.

stressed similarly and it is easy to see when only one of the transistors fails. In this circuit, each normally on transistor (Q) is paired with a normally off transistor ( $Q'$ ). When a Q transistor fails, the large base current that results ( $\approx I_E/2$ ), in combination with the large base resistor ( $R_B$ ), lowers the Q

emitter voltage, eventually causing  $Q'$  to turn on. Monitoring  $I_C$  provides large contrast between a circuit with no failed transistors and a circuit with even a single failed transistor. We are beginning to test such a circuit.

#### SUMMARY

InGaP-emitter HBTs can have much longer lifetimes than AlGaAs-emitter HBTs, so much so that it is difficult to measure the lifetime acceleration parameters  $E_A$  and  $n_J$ . Measurements on some of the poorer wafers have indicated  $E_A \approx 1.2 \text{ eV}$ , and very roughly that  $n_J \sim 1.2$ . The important failure mode is not gradual  $\beta$  drift, but rather sudden  $\beta$  drop to  $\beta \approx 1$ . The large base current for failed devices ( $\approx I_E/2$ ) can be utilized in the design of large reliability test circuits that have enhanced contrast between circuits with and without any failed transistors. MTTFs of wafers with intentional lattice mismatch in the InGaP layer were consistent with those of nominally lattice-matched wafers. However, it may be favorable to be mismatched rather Ga-rich, since such a wafer had one of the best lifetimes. It appears that base current is a more general indicator of current acceleration than emitter current, as the large base currents that can occur in saturation have a current acceleration exponent of  $n_{J_B} \approx 1.8$ .

#### REFERENCES

- [1] T. Takahashi, S. Sasa, A. Kawano, T. Iwai, T. Fujii, *High-reliability InGaP/GaAs HBTs fabricated by self-aligned process*, 1994 IEDM, 191-194, 1994.
- [2] O. Ueda, A. Kawano, T. Takahashi, T. Fujii, S. Sasa, *Solid-State Elec.* **41-10**, 1605-1610, 1997.
- [3] C. Beaulieu, B. Beggs, J. Bennett, J.P.D. Cook, L. Hobbs, T. Lester, B. Oliver, R.K. Surridge, *Degradation modes of GaAs heterojunction bipolar transistors and circuits fabricated in a GaInP emitter technology*, JEDEC GaAs Reliability Workshop, 11-14, 1996.
- [4] T.S. Low, C.P. Hutchinson, P.C. Canfield, T.S. Shirley, R.E. Yeats, J.S.C. Chang, G.K. Essilfie, M.K. Culver, W.C. Whiteley, D.C. D'Avanzo, *Migration from an AlGaAs to an InGaP emitter HBT IC process for improved reliability*, GaAs IC Symposium, 153-156, 1998.
- [5] T. Low, T. Shirley, C. Hutchinson, G. Essilfie, W. Whiteley, B. Yeats, D. D'Avanzo, *InGaP HBT technology for RF and microwave instrumentation*, *Solid-State Elec.*, **43**, 1437-1444, 1999.
- [6] N. Pan, J. Elliot, M. Knowles, D.P. Vu, K. Kishimoto, J.K. Twynam, H. Sato, M.T. Fresina, G.E. Stillman, *High reliability InGaP/GaAs HBT*, *IEEE Elec. Dev. Let.* **19-4**, 115-117, 1999.
- [7] S.L. Delage, S. Cassette, M.A. diForte-Poisson, D. Floriot, E. Chartier, P. Etienne, P. Galtier, J.P. Landesman, *The correlation between material properties and HBT reliability*, GAAS99, Munich, 246-251, 1999.
- [8] F. Ren, C.R. Abernathy, S.N.G. Chu, J.R. Lothian, S.J. Pearton, *The role of hydrogen in current-induced degradation of carbon-doped GaAs/AlGaAs heterojunction transistors*, *Solid-State Elec.* **38**, 1137-1141, 1995.
- [9] S.J. Pearton, C.R. Abernathy, J.W. Lee, F. Ren, C.S. Wu, *Comparison of  $H^+$  and  $He^+$  implant isolation of GaAs-based heterojunction bipolar transistors*, *J. Vac. Sci. Technol.*, **B13**, 15-18, 1995.
- [10] B. Yeats, *Inclusion of topside metal heat spreading in the determination of HBT temperatures by electrical and geometrical methods*, *GaAs IC Symp.*, 59-62, 1999.